Desalination and Water Treatment
www.deswater.com
doi: 10.1080/19443994.2014.966331

56 (2015) 2783–2796
December

Taylor & Francis
Taylor & Francis Group

Nanofiltration of oily wastewater containing salt; experimental studies and optimization using response surface methodology

Hamidreza Abadikhah, Farzin Zokaee Ashtiani*, Amir Fouladitajar

Department of Chemical Engineering, Amirkabir University of Technology, No. 424, Hafez Ave., Tehran, Iran, Tel. +989356568774; email: abadikhah@aut.ac.ir (H. Abadikhah), Tel. +98216454 3124; Fax: +982166405847; email: zokaee@aut.ac.ir (F. Zokaee Ashtiani), Tel. +989124990549; email: fouladi@aut.ac.ir (A. Fouladitajar)

Received 22 February 2014; Accepted 5 September 2014

ABSTRACT

Two separate predictive models were developed for optimization and modeling of the relative permeate flux decline (J/J_0) and Mg ion rejection (%) in nanofiltration (NF) of oily wastewater. Response surface methodology based on central composite design was employed to experimental design and a cumulative study of the effects of various operating parameters such as trans-membrane pressure (TMP), feed flow rate (Q_L), oil concentration (C_{oil}), ion concentration (C_{Mg}), and pH on the NF separation process. Analysis of variance for developed quadratic models exhibited high significance and applicability. The oil and ion concentrations were the most significant factors and their interaction had a prominent effect on both permeate flux and Mg ion rejection. The effect of feed flow rate on the performance was also found to be negligible. The maximum relative permeate flux of 0.86 representing minimum membrane fouling phenomenon was obtained at low levels of input parameters at TMp = 3.4 bar, C_{oil} = 200 mg/L, C_{Mg} = 40 mg/L, and pH 4. Whereas, high rejections were found at high levels of input factors.

Keywords: Membrane; Nanofiltration; Oily wastewater treatment; Rejection; RSM

1. Introduction

Wastewaters containing physical and chemical contaminations such as oil, suspended and dissolved solids are produced as a result of human's activities all over the world. Oil and gas production, manufacturing operations, textile effluent, and food industry are the main reasons of increased polluted waters [1–4]. Due to the large volume of surface discharge, many fatal environmental consequences, including change in vegetation, the loss of surface and underground water recourses, and salt deposition have already been reported [5].

A range of water treatment processes, including biological treatment, flocculation, coagulation, sedimentation, and some other classical methods have been implemented for this global concern, but sever requirements are difficult to be met by these conventional technologies [6–8]. One of the most effective and flexible applications that serves a broad scope in wastewater treatment is presented by membrane separation technology. Membrane processes have offered a number of advantages such as energy saving, wide application in various operations, minimal impact of feed water quality on the output permeate quality, no

*Corresponding author.

need for chemicals, and finally higher impression than other conventional methods [5–10]. However, accumulation of rejected materials on the membrane surface leads to the main disadvantage of membrane processes and membrane fouling [11,12], such a way that approaching to an efficient operation is not possible unless fouling and its effects on separation process are carefully managed [13–23]. Modification of membrane morphology for increasing hydrophilicity [13–15], module design renovation to improve the flow patterns and hydrodynamic effects [16–23], and feed solution pretreatment [24] have been presented to control fouling phenomenon.

Microfiltration (MF) and Ultrafiltration (UF) have been successfully evaluated by a number of studies in oily wastewater treatment [25–28]. However, these processes are unable to meet the required standards in the presence of ionic contaminants [24]. Nanofiltration (NF) has higher abilities in total dissolved solid and COD reduction when compared with MF and UF, and also consumes lower energy in comparison with RO processes. It, therefore, has recently got much more attention as an effective method in wastewater treatment [29–34]. A limited number of studies have reported a cumulative investigation on the full-scale results of NF for oil and ionic concentration diminution during wastewater treatment [5,24], and some other studies have identified NF as an acceptable barrier that removes most of the organic contaminants [35]. Most previous publications have used the conventional experiment methods, in which one independent variable changes at a time while the other parameters remain constant. These classical or conventional experimental approaches involve too many experimental runs and are time consuming, but neglect the effects of possible interactions between the considered parameters of the process which can lead to low efficiency in process optimization [36,37].

Response surface methodology (RSM) is a useful method for modeling and statistical design of experiments which has been increasingly implemented in different applications in the last decade. Yi et al. [38] employed RSM for optimization of anionic polyacrylamide—oil/water emulsion separation from aqueous solution by a modified UF membrane. The application of RSM was presented for copper removal from aqua solution by Cojocaru et al. [39] and Xiarchos et al. [40] for optimization of dead-end and cross-flow ultrafiltration, and also micellar-enhanced ultrafiltration, respectively.

In membrane preparation application, RSM was applied to optimize preparation conditions for fabrication of polydimethylsiloxane (PDMS)/ceramic composite pervaporation [41] and (ABS)/(PVP) NF membrane [42]. Optimization of interfacial polymerization reaction due to formation of a thin-film composite (TFC) membrane was investigated by RSM based on central composite design (CCD) [43], so that membrane performance in the term of rejection and permeate flux were considered as response variables. More recently, RSM was used for developing a predictive model to optimize RO desalination process in which salt concentration, feed flow rate, feed temperature, and trans-membrane pressure (TMP) were investigated to obtain the optimum condition for salt rejection [44]. Based on the mentioned publications, there is a need to study NF of oily wastewater containing salts and analyzing the effects of different operating parameters on the membrane performance.

Accordingly, this paper investigates the applicability of NF membranes in oily wastewater treatment as well as the effects of important operating parameters on the membrane performance. The input variables were TMP, feed flow rate, oil concentration, salt concentration, and pH. Statistical design of experiments was done using RSM based on CCD for modeling and optimization of process. Main proposal of this study was placed on maximization of permeate flux and Mg ion rejection as the desired response functions. Furthermore, predictive models were obtained based on RSM for both permeate flux and Mg ion rejection, revealing the most significant factors and also their interactions.

2. Experimental

2.1. Chemicals and analysis

Magnesium sulfate, $MgSO_4$ (Sigma-Aldrich Co.), gasoil from Tehran refinery, and ultrapure deionized water were used to prepare solutions at desired concentrations. Mixture homogenization and appropriate oily ionic phase distribution were achieved at a mixing rate of 12,000 rpm for 30 min. The surfactant was polyoxyethylene (80) sorbitanmonooleat (Tween 80, Merck) at concentration of 100 mg/L for each feed preparation. To adjust the pH of the feed solution at desired acidic or alkaline condition, hydrochloric acid (HCl, 5 M) aqueous solution, and sodium hydroxide (NaOH, 5 M) solution was used, respectively. dynamic laser scattering method (Nano ZS (red badge) ZEN 3600, Malvern, UK) was used to determine particle size distribution (PSD) of feed solutions, as shown in (Fig. 1). The curves clearly show that no significant diversification has been occurred in the certain period of time during experiments.

The COD values in both feed and permeate solutions were analyzed by conventional potassium

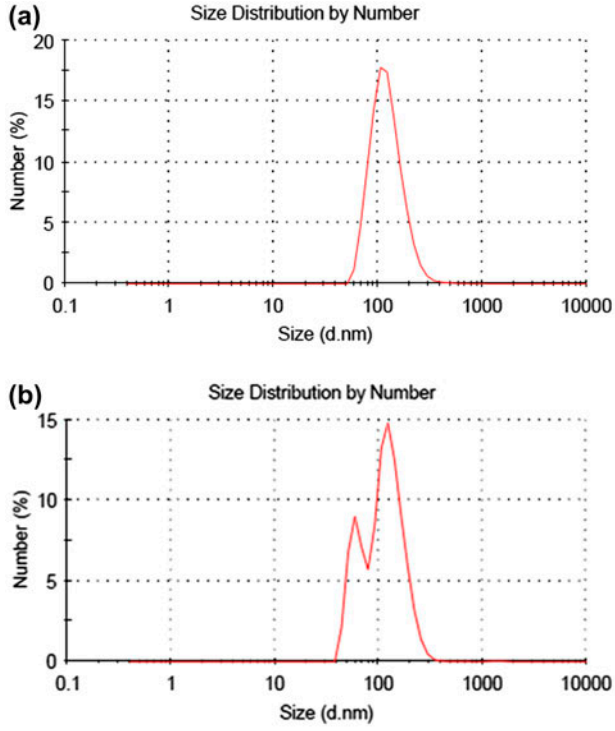

Fig. 1. PSD of feed solution (a): after feed preparation and (b): 2 h after feed preparation.

dichromate oxidation process based on the standard method of EPA 410.4. Atomic absorption spectroscopy procedure was also implemented for the quantitative determination of Mg, and turbidimetric analysis of sulfate was performed based on standard method for the examination of water and wastewater [45].

2.2. Membrane, filtration module, and process apparatus

The performance of a thin-film-composite (TFC) polymer NF membrane (Sepro Membrane Inc, USA) was studied using a transparent flat-sheet membrane module with 50 cm^2 active surface area. The cross-flow membrane module had a $100 \times 50 \times 5$ mm dimension where the module's cross-sectional area for feed flow was 250 mm^2, such a way that the area was completely covered by fluid at all the levels of feed flow rate. The membrane module was designed and made up of two separate plates; more detailed description has been given in previous work [46]. NF experiments were carried out in a bench-scale plant as schematized in Fig. 2.

The stable feed solution containing oily and ionic contaminants was kept in a 10-L tank and was forwarded to the membrane module; for this purpose, a high pressure centrifugal pump, controlled by an inventor was utilized in the designed position. Installation of a needle valve in the retentate line after the membrane module provided adjustment of stream flow rate in the system and exerted a backpressure along the membrane unit. The permeate flow was measured by a digital balance (Sartorius Model GE2120, Germany) connected to a computer. Since the permeate flux in the experiments was very little, the stream specification of input and output flow from the membrane module can be considered similar.

2.3. Process description

Each membrane was initially used for 3 h at same operating conditions using deionized water to prevent any undesirable change in membrane hydraulic resistance during filtration process. All the experiments were carried out under constant temperature by the installation of a cooling water heat exchanger in the feed tank. In every runs, permeate flux measurement was continued until reaching to a constant permeate flux. According to the recommendation of manufacturer and literature data, four principal washing steps were considered to regenerate used membranes: washing with deionized water to remove surface residue, back washing with DI-water at the same TMP, cleaning in place with HCl solution (1 mM, pH 2.7 ± 0.2) for 30 min and NaOH solution (1 mM, pH 11.5 ± 0.3) for 45 min. After membrane recovery, DI water permeability was measured to determine the percentage of membrane regeneration.

2.4. Statistical experimental design

RSM based on five-level-five-factor CCD was applied for simulation and optimization of NF membrane process for oily wastewater treatment. The effects of influential operating parameters including TMP, (X_1), feed flow rate, (X_2), oil concentration, (X_3), salt concentration, (X_4) and pH, (X_5), upon permeate flux, and magnesium rejection as a model for ion contaminants have been studied. The oil rejection values were in the range of 95–98% for all the runs in the set of experiments. Thus, inasmuch as oil rejection values changed in a limited range and showed negligible dependency to input parameters, it has not been selected as a response function. With total number of 50 experiments containing 32 factorial points, 10 axial points, and 8 replicates at the central point have been performed. Mentioned independent variables were coded at three levels in which −1 responds to minimum level, 0 refers to the midlevel, and + 1 is used for maximum value of each parameter. Through the

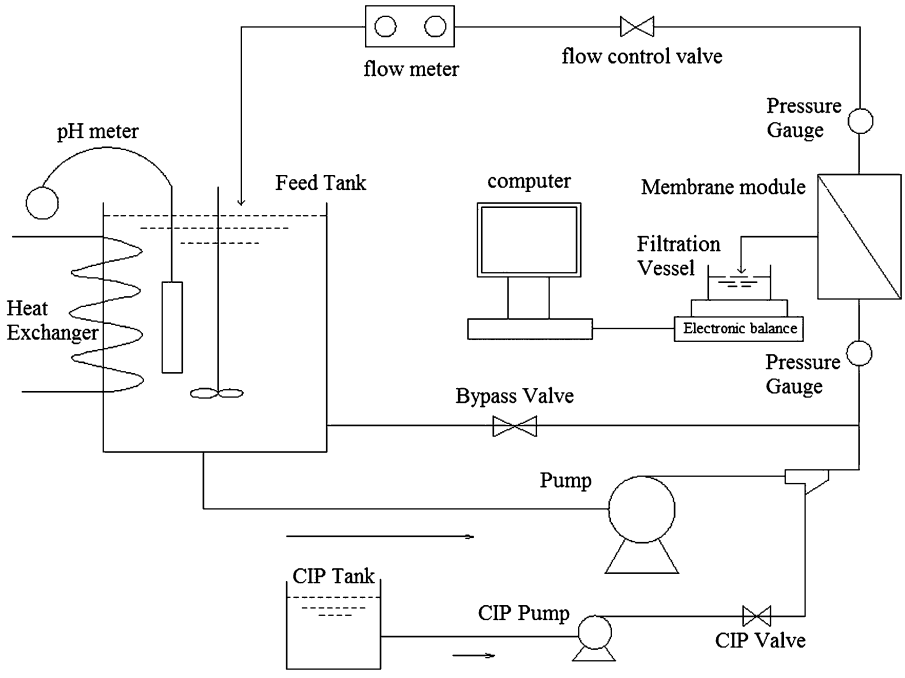

Fig. 2. Schematic diagram of the experimental setup.

CCD method, polynomial regression model can be derived to predict the performance of the process. A general mode of quadratic model is presented as follows:

$$Y = \beta_0 + \sum_{i=1}^{k} \beta_i x_i + \sum_{i=1}^{k} \beta_{ii} x_i^2 + \sum_{i<j}^{k} \beta_{ij} x_i x_j + \xi \quad (1)$$

where Y characterizes the predicted response, x_i and x_j denote the coded levels of independent input variables, β_0 is a constant coefficient, β_i, β_{ii}, and β_{ij} are delineate regression coefficients (main, quadratic, and interaction, respectively), k is the total number of input variables, and ξ is defined as the statistical error. In order to obtain the mentioned regression coefficient in Eq. (1), the ordinary least square [36,37] method is used to minimize the sum of square residual parameter [47]. Design Expert software version 8.0.7.1, was used for the analysis of variance (ANOVA) and response surface.

In the results of COD and oil & grease analysis data, it was clearly determined that the oil rejection ratio of all experiments were higher than 95%, in a way that it was not necessary to consider oil rejection efficiency as the predicted response function in the statistical design of experiments. Therefore, relative flux decline (J/J_0) which is defined as proportion of initial permeate flux to final constant permeate flux and Mg rejection as a model for ionic contaminants rejection were introduced as response functions, and were simulated and optimized using RSM.

Permeate flux, relative permeate flux decline, and Mg rejection were calculated by Eqs. (2)–(4), respectively:

$$J = \frac{M_p}{A \times t} \quad (2)$$

$$Y_1 = \frac{J}{J_0} \quad (3)$$

$$Y_2 = \text{Mg ion rejection} = \left(1 - \frac{c_p}{c_f}\right) \times 100 \quad (4)$$

where J and J_0 refer to the constant and initial permeate flux, L/m^2 h, respectively, M_p is the permeate flow mass, A is the active membrane area, t is the predetermined time of filtration, Y_1 is the relative permeate flux, Y_2 is defined for Mg rejection, and C_p and C_f are the Mg concentration in permeate and feed streams (mg/L), respectively.

3. Results and discussion

3.1. Rejection and relative flux decline studies

For the simulation and optimization of wastewater NF process to determine the effects of every input parameter on both relative permeate flux decline and

rejection factor, two separate predictive response surface models (RS-model) have been developed in the set of experiments. To study the effects of operating variables on relative permeate flux decline, the permeate flux was measured in certain periods of time to reach a stable and constant value. Besides, since the initial flux of membranes was not exactly the same at similar operating conditions, the relative permeate flux was considered. Fig. 3(a) reveals J/J_0 data for all 50 runs in the set of experiments. Permeate flow was collected during filtration period of time and analyzed for oil and ionic contaminants rejection factor. Mg rejection data for all 50 runs has been depicted in Fig. 3(b). As shown in column diagrams, the normalized permeate flux (J/J_0) changed from 0.0379 to 0.902, and value of Mg rejection (%) varied from 56 to 99.8.

3.2. RS model for permeate flux

RSM based on the CCD was applied to study the effects of five operational– influential parameters with all combinations of five factors at three levels: high (+1), low (−1), and the center point (0) replicating eight times. The star or axial points ($\pm\alpha$) with the value of ±1.2 were also considered. The factors involved in this study dealt with the TMP (x_1), feed flow rate (x_2), C_{oil} (x_3), (C_{Mg}) (x_4), and pH (x_5). Five process variables including coded and actual values of factors are shown in Table 1. The data for five coded factors and two responses in the terms of J/J_0 and Mg ion rejection (%) developed by the design of expert software is shown in Table 2.

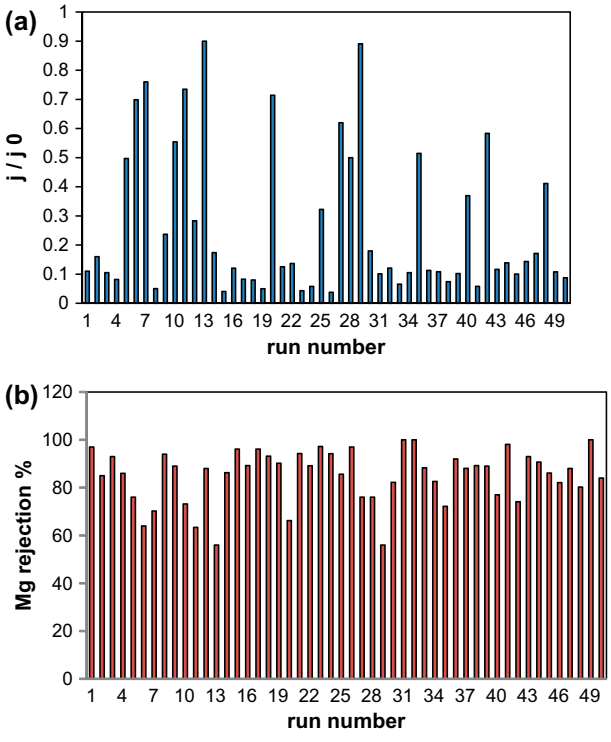

Fig. 3. Results for all 50 experimental runs (a) relative permeate flux decline (J/J_0) and (b) Mg rejection (%).

The modeling and optimization of process was done using a second-order polynomial model including main, quadratic, and interactions terms. As shown in Eq. (5), a reduced quadratic model in terms of coded factors was developed to fit the experimental data for the declined permeate flux.

$$J/J_0\,(Y_1) = 0.13 - 0.036x_1 - 0.24x_3 - 0.087x_4 - 0.056x_5 + 0.026x_1x_3 + 0.076x_3x_4 + 0.043x_3x_5 + 0.19x_3^2 \quad (5)$$

where $-\alpha < x_i < +\alpha$ and $i =$ 1, 3, 4, and 5. This regression model, Eq. (5), can be used for the determination of permeate water flux through NF membrane process for treatment of oily waste water containing salt. It is important to note that statistical student test was used to test the significance of regression coefficients. Using the ANOVA, the significance of the obtained terms was evaluated and the terms with p-value greater than 0.05, known as non-significant terms, were removed from the predictive model. Eq. (5) presents only influential terms and their interactions. According to the results of t-test, the factor x_2 that was referred to feed flow rate was eliminated from final regression equation. Based on Eq. (5), the order of significant factors are as follows:

x_3: first-order main effect of oil concentration; $\geq x_3^2$: oil concentration quadratic order; $\geq x_4$: first-order main effect of Mg concentration; $\geq x_3x_4$: interaction of oil concentration and Mg concentration; $\geq x_5$: first-order main effect of pH; $\geq x_3x_5$: interaction of oil concentration and pH; $\geq x_1$: TMP, first-order main effect of pressure; $\geq x_1x_3$: interaction of TMP and oil concentration.

The ANOVA was applied to examine the adequacy of RS-model for both response functions. In Table 3, ANOVA results for sum of squares (SS), mean squares (MS), degree of freedom (DF), F-value and p-value, residual error, and other error values have been shown. Mathematical methodology to compute statistical estimators (i.e. SS, MS, F-value, p-value, etc.) has been presented in the literature concerning RSM [48]. In statistical view, F-value should be as high as possible, whereas, p-value must be as low as possible. The model F-value of 326.25 and p-value less than 0.0001 imply that the model is significant and there is only 0.01% chance that an error could occur due to noise.

Table 1
Code and level of factors used for CCD

Variables	Symbols	Levels in coded and actual values				
		$-\alpha(-1.2)$	−1	0	+1	$+\alpha(+1.2)$
TMP (bar)	X_1	2.4	3	6	9	9.6
Feed flow rate (L/min)	X_2	0.7	1	2.5	4	4.3
Oil concentration (ppm)	X_3	20	200	1,100	2,000	2,180
Mg concentration (ppm)	X_4	4	40	221.5	403	439
pH	X_5	3.4	4	7	10	10.6

Lack of fit value of 0.74 implies the lack of fit is not significant to the pure error. R^2 value of 0.9845 is quiet close to unity and there is a good agreement between coefficient R^2 and adjusted coefficient, R^2_{adj} (0.9815). Thus, in statistical point of view, this regression model can be applied as an adequate and validate model to predict and simulate NF process within considered independent variables.

The plots of normal probability of residuals and residuals verses the predicted responses for permeate flux decline have been given in Fig. (4). Evaluation of the plot in Fig. 4(a) depicts that the residuals have fallen on a straight line implying normal distribution of errors which confirms sufficiency of the least-square fit. As shown in Fig. 4(b) and (c), there is no obvious pattern or unusual structure, and equal scattering above and below the x-axis proves credibility and adequacy of RS-model for response function. The plot of predicted verses actual values was shown in Fig. 4(d). It can be concluded that an appropriate adaption to the experimental data exists in different levels of input factors, satisfying R^2 value of 0.973.

3.2.1. Effect of TMP

Fig. 5 shows the effects of TMP and C_{oil} factors on relative permeate flux. It can be seen that TMP has a negative effect on relative permeate flux decline. With increasing TMP as the driving force in pressure-driven membranes, the permeate flux was increased, whereas, J/J_0 was obviously declining due to membrane fouling phenomenon. Membrane fouling as a disadvantage of membrane processes occurred in different levels of TMP, but was more significant at higher TMP levels. The reason can be explained by formation of a cake layer containing oil droplets and ionic contaminants on the membrane surface, which acts as an additional resistance to materials diffusion through NF membrane. At higher TMP, the formed cake layer may be tightly compressed, leading to pore blocking and fouling at higher rates. As depicted in Fig. 5, the effect of TMP at lower levels of oil concentration is more significant. For example, enhancement of pressure factor from 3 bar to 9 bar at C_{oil} value of 200 mg/L led to 0.13 decrease in J/J_0 (from 0.62 to 0.49), whereas, at similar pressure enhancement at high level of C_{oil} J/J_0 decreased only 0.02 (from 0.084 to 0.064). It can be concluded that at high C_{oil}, and TMP, more oil droplets can be pushed and pressed into the membrane surface, eventuate to radius decreasing and consequently result in pore constriction and/or blocking. Besides, contour lines show more curvature at higher levels of oil concentrations, presenting more interaction between these two parameters. It can be explained that at higher levels of C_{oil}, increasing TMP leads to more significant fouling due to more oil droplets compaction at the membrane surface. The same behavior was observed for the interaction of TMP and ion concentration, but it was not as significant as TMP and C_{oil} interactions.

3.2.2. Effect of C_{oil} and C_{Mg}

According to the developed RS-model (Eq. 5), it was found that oil concentration was the most influential independent variable, and the interaction between oil and ion concentration was also the most significant interaction. 3-D graph of J/J_0 as a function of C_{oil} and C_{Mg} has been presented in Fig. 6(a). This plot shows that an increase in Coil and C_{Mg} would decrease response function. It has been shown that the effect of Mg concentration is more significant at low oil concentration. The plot also shows that the more permeate flux ratio decline (J/J_0) has been observed at low levels of this factors, because concentration polarization is more significant at higher value of initial feed; Coil and Mg concentration factors form irreversible fouled cake on membrane surface.

Counter-line plot of output response, as a function of pH and Mg concentration, is displayed in Fig. 6(b). As mentioned in the predictive model (Eq. 5), no important interaction was found between these

Table 2
CCD and responses for NF of oily wastewater

	Input parameters					Responses	
Run	TMP X_1 (bar)	Q_L X_2 (L/min)	C_{oil} X_3 (ppm)	C_{Mg} X_4 (ppm)	pH X_5	J/J_0 Y_1	Ion rejection (%) Y_2
1	0	0	0	0	0	0.11	97
2	0	0	0	0	0	0.16	85
3	−1	1	1	−1	1	0.105	93
4	−1	−1	1	1	−1	0.081	86
5	1	1	−1	−1	1	0.497	76
6	−1	−1	−1	−1	1	0.698	64
7	1	1	−1	−1	−1	0.759	70.24
8	−1	1	1	1	1	0.050	94
9	1	−1	−1	1	1	0.236	89
10	1	−1	−1	−1	1	0.554	73.18
11	1	−1	−1	−1	−1	0.735	63.4
12	1	1	−1	1	1	0.283	88
13	−1	1	−1	−1	−1	0.9	56
14	0	0	0	−1.2	0	0.174	86.2
15	1	−1	1	1	1	0.040	96.1
16	0	−1.2	0	0	0	0.120	89.2
17	0	0	0	1.2	0	0.082	96.1
18	1	1	1	−1	1	0.080	93.1
19	0	0	0	0	0	0.05	90.2
20	−1	1	−1	−1	1	0.714	66.2
21	0	1.2	0	0	0	0.125	94.2
22	−1	−1	1	−1	−1	0.136	89.1
23	−1	−1	1	1	1	0.043	97.2
24	0	0	1.2	0	0	0.057	94.2
25	−1	−1	−1	1	1	0.322	85.6
26	1	1	1	1	1	0.037	97
27	0	0	−1.2	0	0	0.62	76
28	1	1	−1	1	−1	0.5	76
29	−1	−1	−1	−1	−1	0.890	56
30	0	0	0	0	0	0.18	82.2
31	0	0	0	0	1.2	0.101	99.8
32	0	0	0	0	0	0.121	99.7
33	1	1	1	1	−1	0.065	88.3
34	1	1	1	−1	−1	0.105	82.6
35	−1	−1	−1	1	−1	0.514	72.2
36	0	0	0	0	0	0.113	92
37	1.2	0	0	0	0	0.108	88.1
38	1	−1	1	−1	1	0.074	89.2
39	−1	−1	1	−1	1	0.101	89
40	−1	1	−1	1	1	0.369	77
41	1	−1	1	1	−1	0.057	98.1
42	−1	1	−1	1	−1	0.583	74.1
43	0	0	0	0	0	0.116	93
44	−1.2	0	0	0	0	0.139	90.7
45	1	−1	1	−1	−1	0.100	86.1
46	−1	1	1	−1	−1	0.143	82.1
47	0	0	0	0	−1.2	0.171	88
48	1	−1	−1	1	−1	0.411	80.2
49	0	0	0	0	0	0.108	99.8
50	−1	1	1	1	−1	0.087	84

Table 3
ANOVA tables and statistical parameters for the reduced regression quadratic RS-model (response: relative permeate flux)

Source	SS	DF	MS	*F*-value	*p*-value
Model	3.05	8	0.38	326.25	<0.0001
x_1-pressure	0.044	1	0.044	37.84	<0.0001
x_3-oil concentration	1.99	1	1.99	1,703.05	<0.0001
x_4-salt concentration	0.26	1	0.26	223.82	<0.0001
x_5-pH	0.11	1	0.11	93.05	<0.0001
x_1x_3	0.021	1	0.021	18.37	0.0001
x_3x_4	0.14	1	0.14	123.17	<0.0001
x_3x_5	0.059	1	0.059	50.45	<0.0001
x_3^2	0.42	1	0.42	360.26	<0.0001
Residual	0.048	41	1.17E-03		
Lack of fit	0.038	34	1.10E-03	0.74	
Pure error	0.01	7	1.49E-03		
Total	3.1	49			
R^2	0.9845				
R^2-adjusted	0.9815				
R^2-predicted	0.9782				
CV (%)	13.21				
Adeq. precision	58.295				

variables. Negative effect of C_{Mg} on J/J_0 has been clearly shown and higher levels of response function, and was obtained at lower levels of ion concentration and pH, respectively.

3.2.3. The effect of pH

Due to its effect on electrostatic forces, pH is one of the most important parameters in the formation of particles aggregation. As illustrated in Fig. 7, J/J_0 decreased with increasing pH value. In addition, higher permeate fluxes were obtained at low pH levels of feed solution. It means that in low pH values, the materials are diffused more easily through porous structure of membranes. The reason of this performance can be described by dissociation of functional groups at low feed solution pH in membrane structure, creating destructive influence on selective layer of TFC membranes [49]. On the other hand, it is believed that oil droplets are dissociated under alkaline pH, and as a result more oil droplets will penetrate through membrane pores causing pore blocking and permeate flux decline.

3.3. RS-model for Mg ion rejection

Second response function, Mg rejection, was modeled and simulated using the same procedure applied for first output function (J/J_0). According to the ANOVA (Table 4), it can be concluded that the developed RS-model is significant from statistical point of view.

Insignificant factors with *p*-values greater than 0.05 were removed from initial model, and the reduced quadratic regression model in the terms of coded factors was developed as follows:

$$\text{Mg rejection}\,(Y_2) = 91.62 + 2.23x_1 + 8.59x_3 + 4.74x_4 + 3.95x - 2.52x_3x_4 - 9.36x_3^2 \quad (6)$$

Subjected to $-\alpha \le x_i \le +\alpha$ for $i = 1$, 3, 4, and 5. As it can be seen in above equation, feed flow rate was eliminated from regression model, whereas, TMP, C_{oil}, C_{Mg}, and pH were introduced as significant input parameters. The model *F*-value of 45.75 demonstrates the model is adequate and there is only 0.01 chance that a model *F*-value could occur due to noise. In addition, the lack of fit value of 0.34 shows the lack of fit is not significant.

Based on statistical estimators such as *F*-value, *p*-value, R^2 value of 0.86, and R^2_{adj} (0.84), the adequacy of Eq. (6) is proved for prediction and determination of Mg rejection (%) of oily wastewater treatment within presented levels of input factors.

3.3.1. Effects of operating parameters on Mg ion rejection

3-D surface plot for interaction of Mg concentration and oil concentration on the basis of developed

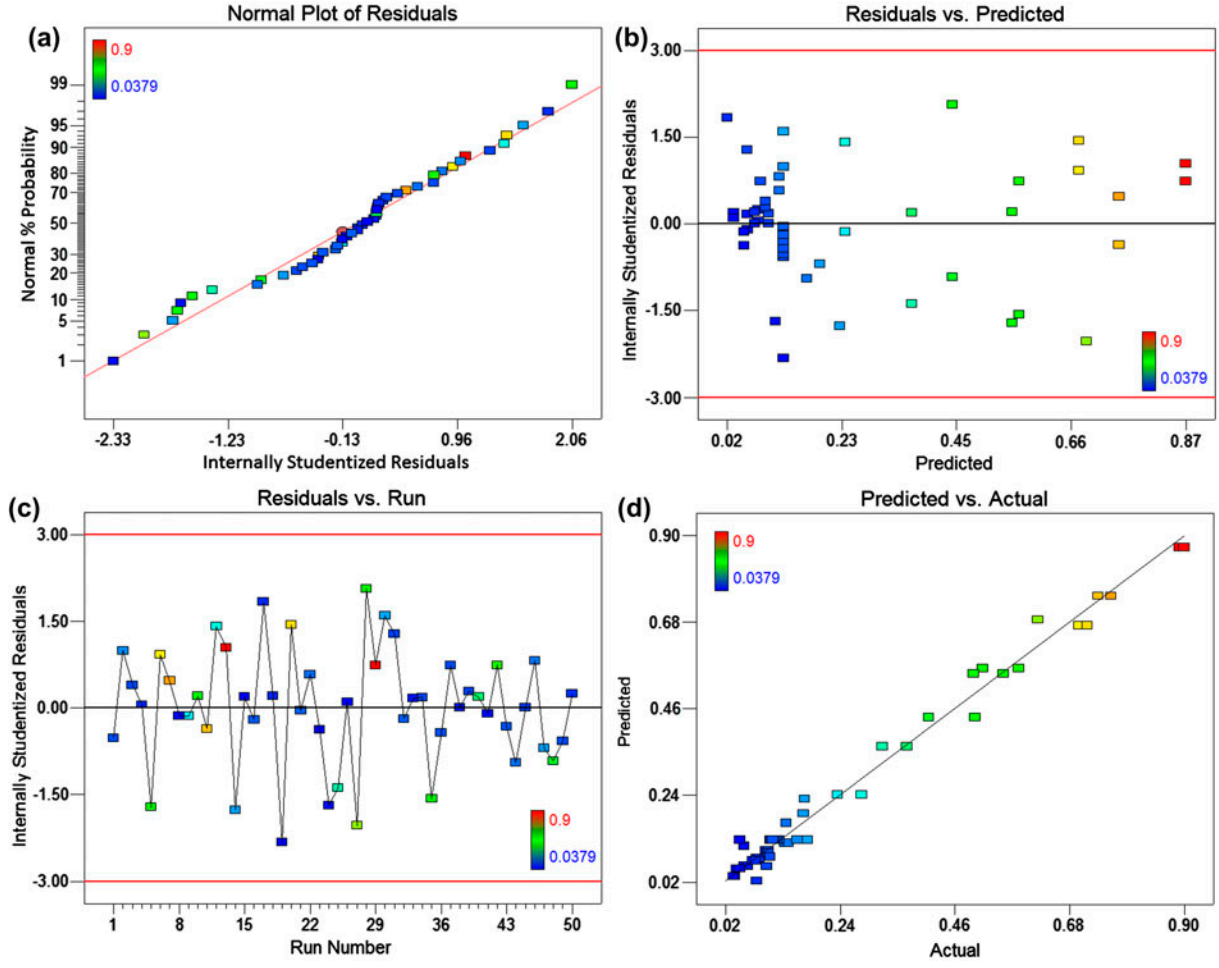

Fig. 4. Residuals plots for CCD design (a, b, and c) and predicted vs. actual values (d).

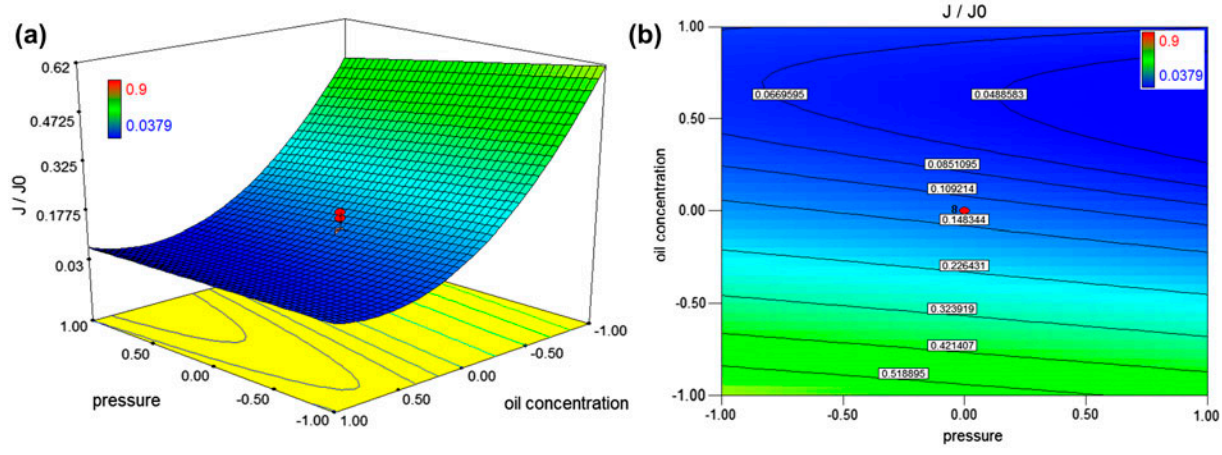

Fig. 5. Relative permeate flux decline (J/J_0) as a function of TMP and C_{oil} factors (a) surface plot and (b) contour map (other variables were held at center levels).

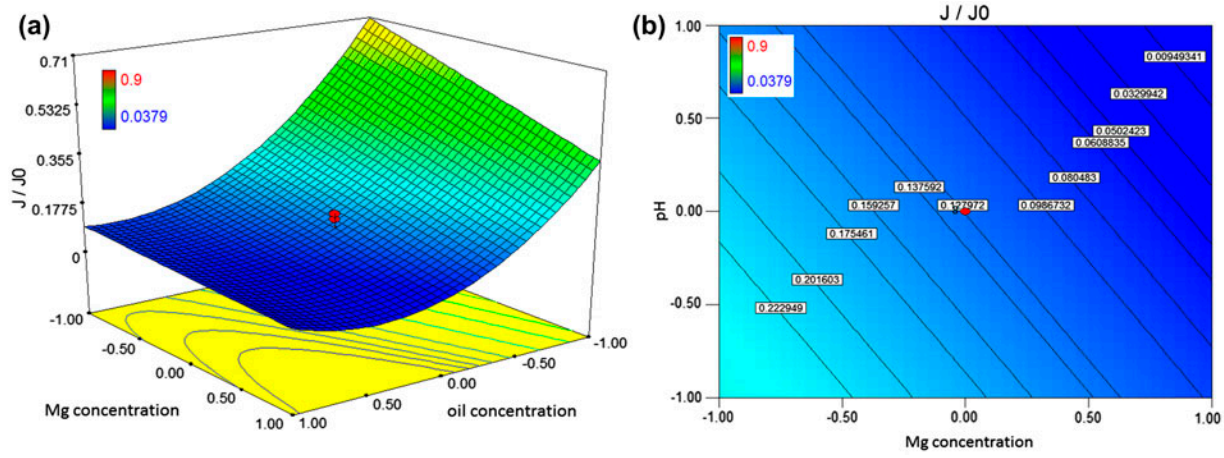

Fig. 6. (a): Relative permeate flux decline (J/J_0) as a function of ion and oil concentration. (b): Contour-lines plot of relative permeate flux as a function of pH and oil concentration.

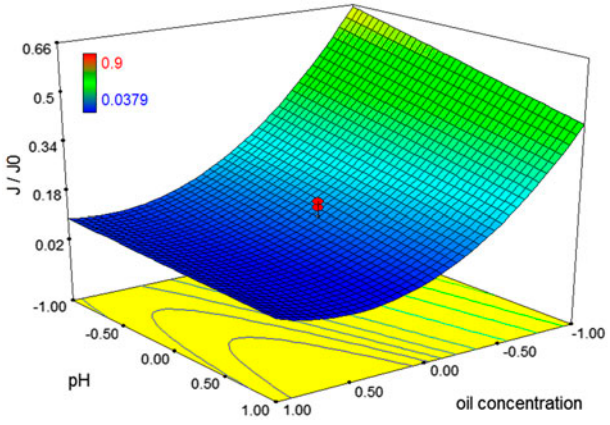

Fig. 7. Relative permeate flux decline (J/J_0) as a function of pH and oil concentration.

Table 4
ANOVA tables and statistical parameters for the reduced regression quadratic RS-model (response: ion rejection)

Source	SS	DF	MS	*F*-value	*p*-value
Model	5,315.34	6	885.89	45.75	<0.0001
Residual	832.69	43	19.36		
Lack of fit	531.95	36	14.78	0.34	0.9838
Pure error	300.75	7	4.30E ± 01		
Cor total	6,148.03	49			

RS-model has been given in Fig. 8(a). This plot describes that these factors have a regressive influence on Mg rejection. As we all know, before the formation of a cake layer above membrane surface, TFC membrane acts as a primary medium for filtration, whereas, after formation of fouling layer, it is considered as primary filtration medium. So, fouling layer has dual effect on NF process; although it may increase materials rejection, permeate flux ratio may decrease. As shown in Fig. 8(a), the effects of salt concentration is more prominent at lower oil concentrations, and also, the effect of oil concentration is found to be more significant at low levels of Mg concentration. For instance, enhancement of C_{Mg} from 40 to 403 (mg/L) at C_{oil} value of 200 (mg/L), resulted in 14.52% increment in the response, while, 4.44% increase was obtained at high oil concentration (2,000 mg/L). This behavior confirms coefficients order of magnitude in regression model for rejection, proving higher influence of oil concentration on fouling and Mg ion rejection.

As illustrated in Fig. 8(b), increasing TMP increased Mg ion rejection. With increasing TMP, convection and mass transfer rate of oil droplets, and ionic contamination from bulk flow to the membrane surface would be increased, leading to the formation of a tight compact fouling layer on the membrane wall. Concentration polarization layer is more significant and considerable at high TMP levels and plays an important role to the ion retention. On the other hand, higher applied pressures force oil droplets and ionic particles to pass through the membrane pores, causing pore blocking issue. Therefore, one can conclude that increment of TMP results in a more significant concentration polarization phenomenon, in which it not only reduces the relative permeate flux (J/J_0) but also increases Mg rejection.

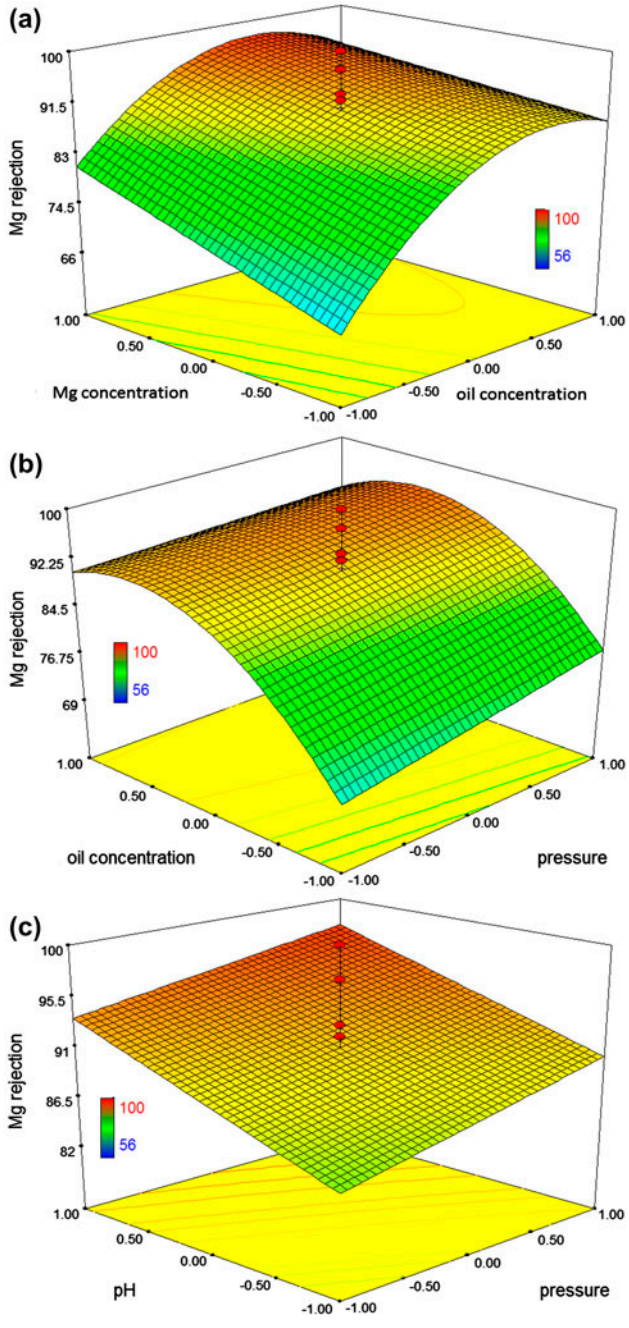

Fig. 8. Ion rejection surface plots as a function of (a) Mg and oil concentration, (b) oil concentration and TMP, and (c) pH and TMP.

For determining the effect of pH on rejection response function, the 3-D surface plot of Mg rejection (%) as a function of pH and pressure is presented in Fig. 8(c). It indicates that increasing pH and TMP would enhance the Mg rejection. In other words, the higher the pH, the higher the Mg ion rejection. This is due to the fact that Zeta potential or charge density at the membrane surface changes as a function of pH. It becomes more negative when the pH of the solution attains an alkaline pH. Therefore, by increasing the pH value, charge density at the membrane surface arises, and as a result, more negatively charged ions are rejected by membrane according to the Donnan exclusion [49]. Since the electrical nature of the solution must remain at neutral condition, more retention for positively charged ions is achieved.

3.4. Process optimization

Process optimization for both relative permeate flux decline (J/J_0) and Mg ion rejection were calculated by RSM model. As mentioned earlier, two separate predictive models were presented for response functions. In the case of (J/J_0), the optimal operating condition that provides minimum fouling effects is expressed as follow: TMP = 3(bar), C_{oil} = 200 (mg/L), C_{Mg} = 40 (mg/L), and pH 4. Under these optimum conditions, J/J_0 value was obtained at 0.86. For the second response, Mg ion rejection (%), higher levels of operating parameters were derived as optimum conditions: TMP value of 5.22 (bar), C_{oil} value of 1,342 (mg/L), C_{Mg} value of 380 (mg/L), and the pH value of 9.9 led to maximum Mg ion rejection close to 99% obviously. In practical cases, maximization of both responses is favorable. Optimization of NF process to achieve maximum J/J_0 and Mg ion rejection eventuates to 0.53 and 75.96% for relative permeate flux and Mg rejection, respectively. Actual operating parameters, as well as the predictive response, and experimental response at optimal points have been demonstrated in Table 5.

Table 5
Optimal condition in terms of the actual operating condition and the predicted and experimental responses

TMP (bar)	C_{oil} (ppm)	C_{Mg} (ppm)	pH	Flux predicted (J/J_0)	Rejection predicted (%)	Flux experimental (J/J_0)	Rejection experimental (%)
3	222	403	4.5	0.53	75.9	0.48 ± 0.02	73.7 ± 0.2

4. Conclusions

RSM based on CCD was applied to study the effects of operating process parameters including TMP, feed flow rate, ion concentration, ion concentration, and pH on NF of oily wastewaters containing salt. Optimization and modeling of relative permeate flux (J/J_0) and Mg ion rejection (%) as the desired response functions were successfully implemented, and two separate significant predictive models were developed for output functions. Oil concentration and ion concentration were not only found to be the most significant factors on J/J_0 and rejection, but they also showed great interaction. Some other interactions were found between TMP–C_{oil} and C_{oil}–pH, but no other influential interaction was observed for the Mg ion rejection model. Feed flow rate showed insignificant influence on responses and was eliminated form predictive models. Higher values of J/J_0 function were obtained at low levels of TMP, C_{oil}, and C_{Mg} due to weaker fouling layer on the membrane surface. pH revealed negative effect on J/J_0, whereas it was positive for Mg ion rejection. In addition, optimum operating conditions in order to maximizethe response functions were calculated by RSM and confirmed experimentally. Thus, RSM was successfully applied for evaluating the importance of operating process factors and approaching to the optimal NF process condition for wastewater treatment.

Nomenclature

Y	—	predicted response
x_i and x_j	—	coded levels of independent input variables
β_0	—	value of fixed response (offset term) at the central point
β_i β_{ii}, and β_{ij}	—	regression coefficients (main, quadratic, and interaction, respectively)
k	—	the total number of input variables
ξ	—	statistical error
J	—	final constant permeate flux, L/m^{2}h
J_0	—	initial permeate flux, L/m^{2}h
M_p	—	permeate flow mass
A	—	active membrane area
t	—	predetermined time of filtration
y	—	the relative permeate flux decline
R	—	function for Mg rejection
C_p	—	mg concentration in permeate stream, mg/L
C_f	—	mg concentration in feed streams, mg/L
Y_1	—	predicted response for relative permeate flux
Y_2	—	predicted response for Mg rejection

References

[1] X. Qu, P.J.J. Alvarez, Q. Li, Applications of nanotechnology in water and wastewater treatment, Water Res. 47 (2013) 3931–3946.

[2] A. Fakhru'l-Razi, A. Pendashteh, L.C. Abdullah, D.R.A. Biak, S.S. Madaeni, Z.Z. Abidin, Review of technologies for oil and gas produced water treatment, J. Hazard. Mater. 170 (2009) 530–551.

[3] V.V. Goncharuk, A.A. Kavitskaya, M.D. Skil'skaya, Nanofiltration in drinking water supply, J. Water Chem. Technol. 33 (2011) 37–54.

[4] M. Cheryan, N. Rajagopalan, Membrane processing of oily streams. Wastewater treatment and waste reduction, J. Membr. Sci. 151 (1998) 13–28.

[5] S. Mondal, S. Wickramasinghe, Produced water treatment by nanofiltration and reverse osmosis membranes, J. Membr. Sci. 322 (2008) 162–170.

[6] N.A. Gardner, Flotation techniques applied to the treatment of effluents, Effluent Water Treat. J. 12 (1972) 82–88.

[7] H. Huang, K. Schwab, J.G. Jacangelo, Pretreatment for low pressure membranes in water treatment: A review, Environ. Sci. Technol. 43 (2009) 3011–3019.

[8] J.-D. Lee, S.-H. Lee, M.-H. Jo, P.-K. Park, C.-H. Lee, J.-W. Kwak, Effect of coagulation conditions on membrane filtration characteristics in coagulation−microfiltration process for water treatment, Environ. Sci. Technol. 34 (2000) 3780–3788.

[9] Y. Pan, T. Wang, H. Sun, W. Wang, Preparation and application of titanium dioxide dynamic membranes in microfiltration of oil-in-water emulsions, Sep. Purif. Technol. 89 (2012) 78–83.

[10] J. Cui, X. Zhang, H. Liu, S. Liu, K.L. Yeung, Preparation and application of zeolite/ceramic microfiltration membranes for treatment of oil contaminated water, J. Membr. Sci. 325 (2008) 420–426.

[11] A. Fouladitajar, F. Zokaee Ashtiani, A. Okhovat, B. Dabir, Membrane fouling in microfiltration of oil-in-water emulsions; a comparison between constant pressure blocking laws and genetic programming (GP) model, Desalination 329 (2013) 41–49.

[12] Y. Pan, W. Wang, T. Wang, P. Yao, Fabrication of carbon membrane and microfiltration of oil-in water emulsion: An investigation on fouling mechanisms, Sep. Purif. Technol. 57 (2007) 388–393.

[13] J.-e. Zhou, Q. Chang, Y. Wang, J. Wang, G. Meng, Separation of stable oil–water emulsion by the hydrophilic nano-sized ZrO_2 modified Al_2O_3 microfiltration membrane, Sep. Purif. Technol. 75 (2010) 243–248.

[14] S.P. Sun, T.A. Hatton, S.Y. Chan, T.-S. Chung, Novel thin-film composite nanofiltration hollow fiber membranes with double repulsion for effective removal of emerging organic matters from water, J. Membr. Sci. 401–402 (2012) 152–162.

[15] W. Chen, J. Peng, Y. Su, L. Zheng, L. Wang, Z. Jiang, Separation of oil/water emulsion using Pluronic F127 modified polyethersulfone ultrafiltration membranes, Sep. Purif. Technol. 66 (2009) 591–597.

[16] G.N. Vatai, D.M. Krstic, W. Höflinger, A.K. Koris, M.N. Tekic, Combining air sparging and the use of a static mixer in cross-flow ultrafiltration of oil/water emulsion, Desalination 204 (2007) 255–264.

[17] N. Moulai-Mostefa, O. Akoum, M. Nedjihoui, L. Ding, M.Y. Jaffrin, Comparison between rotating disk and vibratory membranes in the ultrafiltration of oil-in-water emulsions, Desalination 206 (2007) 494–498.
[18] D.M. Krstić, W. Höflinger, A.K. Koris, G.N. Vatai, Energy-saving potential of cross-flow ultrafiltration with inserted static mixer: Application to an oil-in-water emulsion, Sep. Purif. Technol. 57 (2007) 134–139.
[19] Z.F. Cui, S. Chang, A.G. Fane, The use of gas bubbling to enhance membrane processes, J. Membr. Sci. 221 (2003) 1–35.
[20] R.J. Wakeman, C.J. Williams, Additional techniques to improve microfiltration, Sep. Purif. Technol. 26 (2002) 3–18.
[21] G. Ducom, H. Matamoros, C. Cabassud, Air sparging for flux enhancement in nanofiltration membranes: Application to O/W stabilised and non-stabilised emulsions, J. Membr. Sci. 204 (2002) 221–236.
[22] A. Fouladitajar, F. Zokaee Ashtiani, H. Rezaei, A. Haghmoradi, A. Kargari, Gas sparging to enhance permeate flux and reduce fouling resistances in cross flow microfiltration, J. Ind. Eng. Chem. 20 (2014) 624–632.
[23] K. Scott, R.J. Jachuck, D. Hall, Crossflow microfiltration of water-in-oil emulsions using corrugated membranes, Sep. Purif. Technol. 22–23 (2001) 431–441.
[24] E.-S. Kim, Y. Liu, M.G. Gamal El-Din, The effects of pretreatment on nanofiltration and reverse osmosis membrane filtration for desalination of oil sands process-affected water, Sep. Purif. Technol. 81 (2011) 418–428.
[25] I.W. Cumming, R.G. Holdich, I.D. Smith, The rejection of oil by microfiltration of a stabilised kerosene/water emulsion, J. Membr. Sci. 169(1) (2000) 147–155.
[26] T.C. Arnot, R.W. Field, A.B. Koltuniewicz, Cross-flow and dead-end microfiltration of oily-water emulsions, J. Membr. Sci. 169 (2000) 1–15.
[27] J.C. Campos, R.M.H. Borges, A.M. Oliveira Filho, R. Nobrega, G.L. Sant'Anna Jr., Oilfield wastewater treatment by combined microfiltration and biological processes, Water Res. 36 (2002) 95–104.
[28] M. Zare, F. Zokaee Ashtiani, A. Fouladitajar, CFD modeling and simulation of concentration polarization in microfiltration of oil–water emulsions; Application of an Eulerian multiphase model, Desalination 324 (2013) 37–47.
[29] E. Park, S.M. Barnett, Oil/water separation using nanofiltration membrane technology, Sep. Sci. Technol. 36 (2001) 1527–1542.
[30] Z. László, S. Kertész, E. Mlinkovics, C. Hodúr, Dairy waste water treatment by combining ozonation and nanofiltration, Sep. Sci. Technol. 42 (2007) 1627–1637.
[31] Z. László, S. Kertész, S. Beszédes, Z. Hovorka-Horváth, G. Szabó, C. Hodúr, Effect of preozonation on the filterability of model dairy waste water in nanofiltration, Desalination 240 (2009) 170–177.
[32] H. Peng, K. Volchek, M. MacKinnon, W.P. Wong, C.E. Brown, Application on to nanofiltration to water management options for oil sands operation, Desalination 170 (2004) 137–150.
[33] M.J.W. Frank, J.B. Westerink, A. Schokker, Recycling of industrial waste water by using a two-step nanofiltration process for the removal of colour, Desalination 145 (2002) 69–74.
[34] M.S.H. Bader, Nanofiltration for oil-fields water injection operations: Analysis of concentration polarization, Desalination 201 (2006) 106–113.
[35] V. Yangali-Quintanilla, S.K. Maeng, T. Fujioka, M. Kennedy, G. Amy, Proposing nanofiltration as acceptable barrier for organic contaminants in water reuse, J. Membr. Sci. 362 (2010) 334–345.
[36] D.C. Montgomery, Design and Analysis of Experiment, second ed., John Wiley & Sons, New York, NY, 2001.
[37] D.C. Montgomery, Response Surface Methods and other Approaches to Process Optimization Design and Analysis of Experiments, fifth ed., John Wiley & Sons, New York, NY, 2001, p. 427.
[38] X.S. Yi, W.X. Shi, S.L. Yu, C. Ma, N. Sun, S. Wang, L.M. Jin, L.P. Sun, Optimization of complex conditions by response surface methodology for APAM—Oil/water emulsion removal from aqua solutions using nano-sized TiO_2/Al_2O_3 PVDF ultrafiltration membrane, J. Hazard. Mater. 193 (2011) 37–44.
[39] C. Cojocaru, G. Zakrzewska-Trznadel, Response surface modeling and optimization of copper removal from aqua solutions using polymer assisted ultrafiltration, J. Membr. Sci. 298 (2007) 56–70.
[40] I. Xiarchos, A. Jaworska, G. Zakrzewska-Trznadel, Response surface methodology for the modelling of copper removal from aqueous solutions using micellar-enhanced ultrafiltration, J. Membr. Sci. 321 (2008) 222–231.
[41] F. Xiangli, W. Wei, Y. Chen, W. Jin, N. Xu, Optimization of preparation conditions for polydimethylsiloxane (PDMS)/ceramic composite pervaporation membranes using response surface methodology, J. Membr. Sci. 311 (2008) 23–33.
[42] S.S. Madaeni, N. Arast, F. Rahimpour, Y. Arast, Fabrication optimization of acrylonitrile butadiene styrene (ABS)/polyvinylpyrrolidone (PVP) nanofiltration membrane using response surface methodology, Desalination 280 (2011) 305–312.
[43] A. Idris, F. Kormin, M.Y. Noordin, Application of response surface methodology in describing the performance of thin film composite membrane, Sep. Purif. Technol. 49 (2006) 271–280.
[44] A. Salahi, I. Noshadi, R. Badrnezhad, B. Kanjilal, T. Mohammadi, Nano-porous membrane process for oily wastewater treatment: Optimization using response surface methodology, J. Environ. Chem. Eng. 1 (2013) 218–225.
[45] L.S. Clesceri, A.E. Greenberg, A.D. Eaton, Standard Methods for the Examination of Water and Wastewater, APHA, AWWA and WEF, Washington, DC, 1998.
[46] H. Rezaei, F. Ashtiani, A. Fouladitajar, Effects of operating parameters on fouling mechanism and membrane flux in cross-flow microfiltration of whey, Desalination 274 (2011) 262–271

[47] M. Khayet, M.N.A. Seman, N. Hilal, Response surface modeling and optimization of composite nanofiltration modified membranes. J. Membr. Sci. 349 (2010) 113–122.
[48] J. Landaburu-Aguirre, E. Pongrácz, P. Perämäki, R.L. Keiski, Micellar-enhanced ultrafiltration for the removal of cadmium and zinc: Use of response surface methodology to improve understanding of process performance and optimisation, J. Hazard. Mater. 180 (2010) 524–534.
[49] D. Nanda, K.-L. Tung, Y.-L. Li, N.-J. Lin, C.-J. Chuang, Effect of pH on membrane morphology, fouling potential, and filtration performance of nanofiltration membrane for water softening, J. Membr. Sci. 349 (2010) 411–420.